Swiss J Geosci (2010) 103:15–32
DOI 10.1007/s00015-010-0004-6

Brittle faulting in the Rawil depression: field observations from the Rezli fault zones, Helvetic nappes, Western Switzerland

Deta Gasser · Neil S. Mancktelow

Received: 10 January 2009 / Accepted: 2 December 2009 / Published online: 28 May 2010

Abstract The Helvetic nappes in the Swiss Alps form a classic fold-and-thrust belt related to overall NNW-directed transport. In western Switzerland, the plunge of nappe fold axes and the regional distribution of units define a broad depression, the Rawil depression, between the culminations of Aiguilles Rouge massif to the SW and Aar massif to the NE. A compilation of data from the literature shows that, in addition to thrusts related to nappe stacking, the Rawil depression is cross-cut by four sets of brittle faults: (1) NE-SW striking normal faults, (2) NW-SE striking normal faults and joints, (3) ENE-WSW striking and (4) WNW-ESE striking normal plus dextral oblique-slip faults. Fault set 1 was probably initiated during sedimentation and reactivated during nappe stacking, whereas the other fault sets formed after emplacement of the Helvetic nappes. We studied in detail two well-exposed parallel fault zones from set 4, the Rezli fault zones (RFZ) in the Wildhorn Nappe. They are SW-dipping oblique-slip faults with a total displacement across the two fault zones of ~200 m vertically and ~680 m horizontally. The fault zones crosscut four different lithologies: limestone, intercalated marl and limestone, marl and sandstone. The internal architecture of the RFZ strongly depends on the lithology in which they developed. In the limestones, they consist of extension veins, stylolites, cataclasites and cemented gouge, in the intercalated marls and limestones of shear zones, brittle fractures and chaotic folds, in the marls of anastomosing shear zones, pressure solution seams and veins and in the sandstones of coarse breccia, brittle faults and extension veins. Sharp, discrete fault planes within the broader fault zones cross-cut all lithologies. Fossil fault zones in the Rezli area can act as a model for studying processes still occurring at deeper levels in this seismically active region.

Keywords Fault zone architecture · Oblique-slip faulting · Brittle deformation · Wildhorn nappe · Helvetic nappes · Rawil depression

Editorial handling: A. G. Milnes.

D. Gasser (✉)
Department of Earth Sciences, University of Graz, Universitätsplatz 2, 8010 Graz, Austria
e-mail: deta.gasser@uni-graz.at

N. S. Mancktelow
Geological Institute, ETH Zürich, 8092 Zürich, Switzerland

Introduction

Deformation in the upper crust is commonly localised in brittle fault zones (e.g. Sibson 1977; Scholz 1988; Snoke et al. 1998). Such fault zones are complex structures composed of variably deformed wall rocks and discrete fractures (e.g. Kurz et al. 2008; Braathen et al. 2009). Many conceptual models for the geometry of such fault zones and the processes that led to their formation have been proposed in the literature (e.g. Sibson 1986a, b, 1990, 1994; Caine et al. 1996; Childs et al. 1996; Crider and Peacock 2004; Braathen et al. 2009). These models are based on detailed descriptions of natural examples of brittle fault zones studied in two (or, in some cases, three dimensions) at different scales (e.g. Kelly et al. 1998; Faulkner et al. 2003; Tarasewicz et al. 2005; Bonson et al. 2007; Hausegger et al. 2009). However, such descriptions are often limited by the poor exposure of brittle fault zones at the Earth's surface. Products of brittle faulting often weather more easily than the surrounding rocks and are therefore hidden below narrow trenches or valleys and

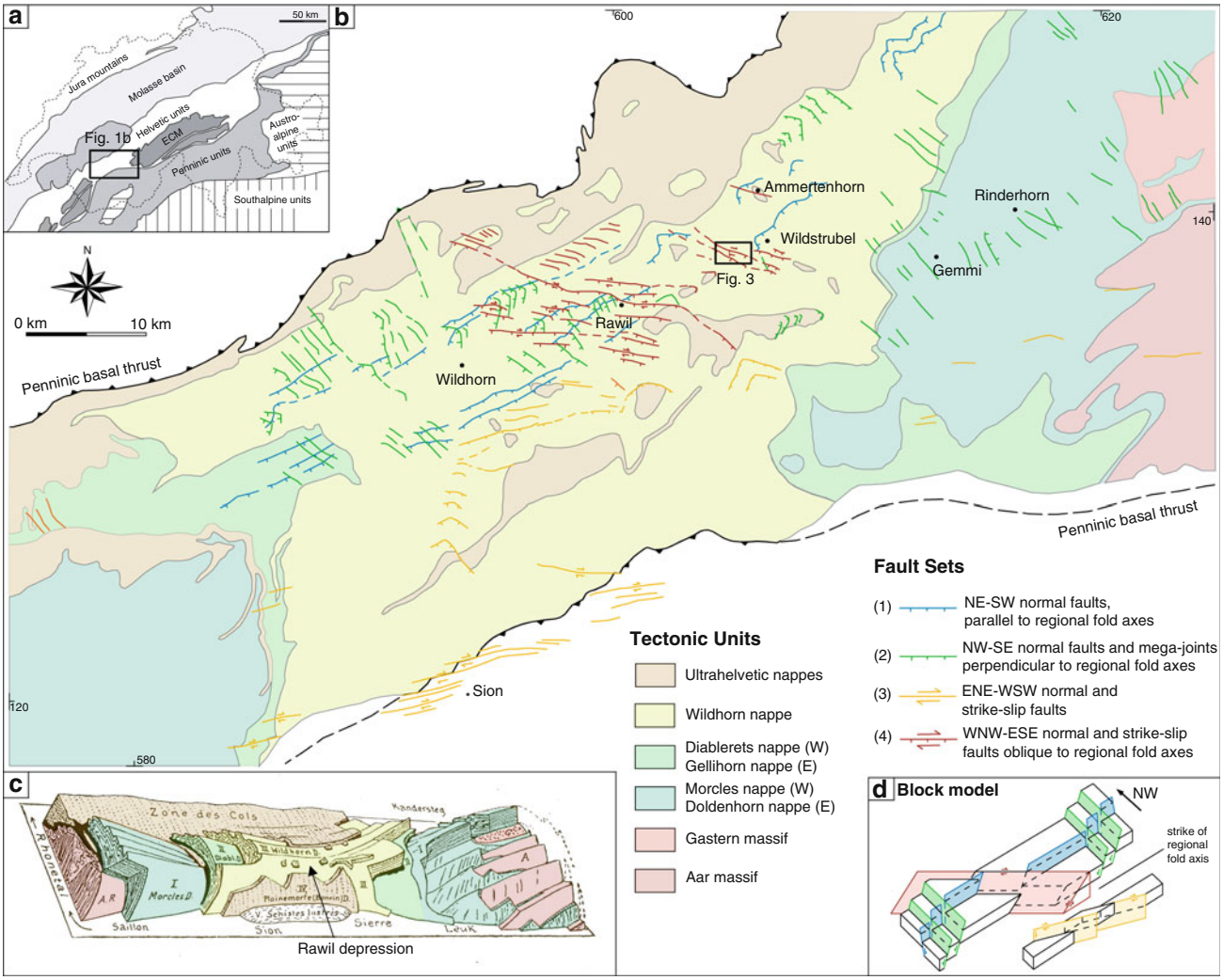

Fig. 1 **a** Tectonic sketch map of Switzerland with the location of the study area indicated. **b** Compilation of fault data from the literature for the Helvetic nappes in the Rawil depression. **c** 3-D sketch of the Helvetic nappes in the Rawil depression after Heim (1921, Vol. II.1, Fig. 147). **d** Schematic block model indicating the orientation, sense of displacement and relationships between the different fault sets

covered by debris or vegetation. The Helvetic nappes of western Switzerland are cross-cut by various brittle faults (Fig. 1; e.g. Pavoni 1980; Franck et al. 1984; Huggenberger and Aebli 1989; Ustaszewski and Pfiffner 2008). Many of these faults are very well exposed in this high-alpine environment, particularly when only recently uncovered from below glaciers that have retreated dramatically in the last decades. Moreover, the faults often cross-cut a wide range of rock types, allowing detailed field studies of the internal fault zone architecture[1] in different host rocks.

In this study, we first present a compilation of normal, oblique–normal and strike-slip fault data from the literature for the western Helvetic nappes in the Rawil depression. The faults could be subdivided into four groups on the basis of their orientation, sense of displacement and age of activity. We then present the results of a thorough field investigation of two parallel, exceptionally well-exposed fault zones in the Rawil depression: the Rezli fault zones (RFZ). We conducted detailed field mapping at a scale of 1:5,000 and constructed two profiles through the fault zones. The RFZ cut through layered and folded Mesozoic sediments of the Helvetic Wildhorn nappe. They therefore cut through various lithologies, with the internal structure of the fault zones varying depending on the lithology in which they developed. We compare the internal structure of the RFZ within these different lithologies to published models of brittle fault zone architecture. Finally, we also discuss the implications of our findings on the regional interpretation of Neogene brittle tectonics (post-nappe-stacking brittle faulting) in the Rawil depression.

[1] For a discussion of the usage of the term "architecture" related to fault zones see Peacock (2008) and Wilson (2008). We agree with the latter author, and continue to use the term in the sense of Caine et al. (1996), among many others.

Geological setting: the Rawil depression

The Helvetic nappes of western Switzerland consist of several internally deformed and imbricated thrust sheets of layered Mesozoic and Tertiary sedimentary rocks. They are preserved in a large-scale depression in the underlying crystalline basement, the so-called Wildstrubel or Rawil depression (Fig. 1; cf. Ramsay 1981, 1989; Burkhard 1988a, b; Dietrich 1989a, b; Dietrich and Casey 1989; Levato et al. 1994). In the centre of the depression, the structurally highest Wildhorn nappe is exposed. This nappe consists of a lower (and southern) part of Jurassic rocks imbricated into smaller thrust sheets, and an upper (northern) part of folded Cretaceous and Eocene rocks. The Wildhorn nappe is underlain by the Gellihorn nappe to the northeast and the Diablerets nappe to the southwest, with the Gellihorn nappe in turn underlain by the Doldenhorn nappe and the Diablerets nappe by the Morcles nappe. There is no exposed connection between the Gellihorn and Diablerets nappes or between the Doldenhorn and Morcles nappes, but their corresponding positions in the structural pile suggest they are probably continuous at depth. The Helvetic nappes are overlain by small remnants of Ultrahelvetic nappes, which are overthrust by Penninic units (e.g. Burkhard 1988a). A schematic 3-D sketch of the Rawil depression and its internal tectonostratigraphy is given in Heim (1921), drawn by Arbenz on the basis of Lugeon's mapping, and is reproduced in Fig. 1c.

Several important problems concerning the geometry and origin of the Rawil depression remain unresolved. Published projections and contour line constructions suggest that the basement rocks below the depression may go down to a depth of 4–6 km below sea level (Burkhard 1988a, b; Dietrich 1989a; Levato et al. 1994). Burkhard (1988b) considered the overall distribution of tectonic units and constructed a symmetric depression with the centre lying in the region of the Rawil pass (Fig. 1b), whereas Dietrich (1989a) considered the regional plunge of fold axes and constructed an asymmetric depression with the centre lying between Wildstrubel and Gemmi pass (Fig. 1b). According to Burkhard (1988a, b), the Aiguilles Rouge and Aar massifs were exhumed as large-scale antiforms above thrusts in the underlying crystalline basement, with the Rawil depression formed as the result of a deep-seated dextral wrench zone connecting the slightly offset Aiguilles Rouge and Aar massifs. In contrast, Dietrich (1989a, b) and Ramsay (1989) considered the Rawil depression to be the result of a change in the thrusting direction from top-to-N during early stages of the Alpine collision to top-to-W during a late stage of the Alpine collision. According to them, this late-stage movement led to fold-axis-parallel stretching and large-scale depressions and culminations, such as the Rawil depression and Aiguilles Rouge and Aar culminations.

Compilation of fault data for the Rawil depression

Besides numerous thrusts associated with nappe emplacement (not shown on Fig. 1b), the Helvetic nappes in the Rawil depression are cross-cut by many different brittle faults that show a range of kinematics from normal, through oblique–normal, to strike-slip. There is considerable information on these faults available in the literature, though unfortunately still without any modern analysis of fault slip data on a regional scale. Figure 1b shows our compilation of such normal, oblique–normal and strike-slip fault data from existing geological maps and the literature (Schaub 1936; Furrer 1938, 1956; Furrer and Hügi 1952; Badoux 1959, 1962; Pavoni 1980; Franck et al. 1984; Burkhard 1986; Masson 1988; Dietrich 1989a; Huggenberger and Aebli 1989; Steck 1999). A fault map for the same region was published by Ustaszewski and Pfiffner (2008). This map differs from ours because it is based on an analysis of lineaments from aerial photographs, whereas our map is based on geological maps and descriptions in the literature that were derived directly from field observations. A comparison of the two maps shows that not every lineament visible on aerial photos has been previously recognised in the field and recorded on geological maps, and not every fault recognised in the field was discernible on aerial photographs. However, overall the general distribution and trends of faults on both maps are comparable.

We distinguish four different sets of such faults based on their orientation, sense of displacement and age of formation (Figs. 1b, c, 2). (1) NE-SW striking normal faults with SE-side down sense of movement that strike parallel to the regional fold axis trend (Fig. 2a). These normal faults developed all along the northern part of the Helvetic nappes. Single fault segments can be followed over a distance of several kilometres. Some of the normal faults probably already formed as syn-sedimentary normal faults and were reactivated during subsequent thrusting and folding (Günzler-Seiffert 1952; Burkhard 1988a; Huggenberger and Aebli 1989). (2) NW-SE striking conjugate normal faults with both NE- and SW-side down sense of movement that strike perpendicular to the regional fold axis trend (Fig. 2b). These normal faults are accompanied by numerous joints and extension veins that are common throughout the Helvetic nappes (the Type III late tectonic tensile veins of Burkhard and Kerrich 1988). The faults cut through the Helvetic nappe boundaries and belong to a phase of extension parallel to the fold axes in the western Helvetic nappes (Huggenberger and Aebli 1989; Dietrich 1989a; Ramsay 1989; Ustaszewski et al. 2007). (3) Steep

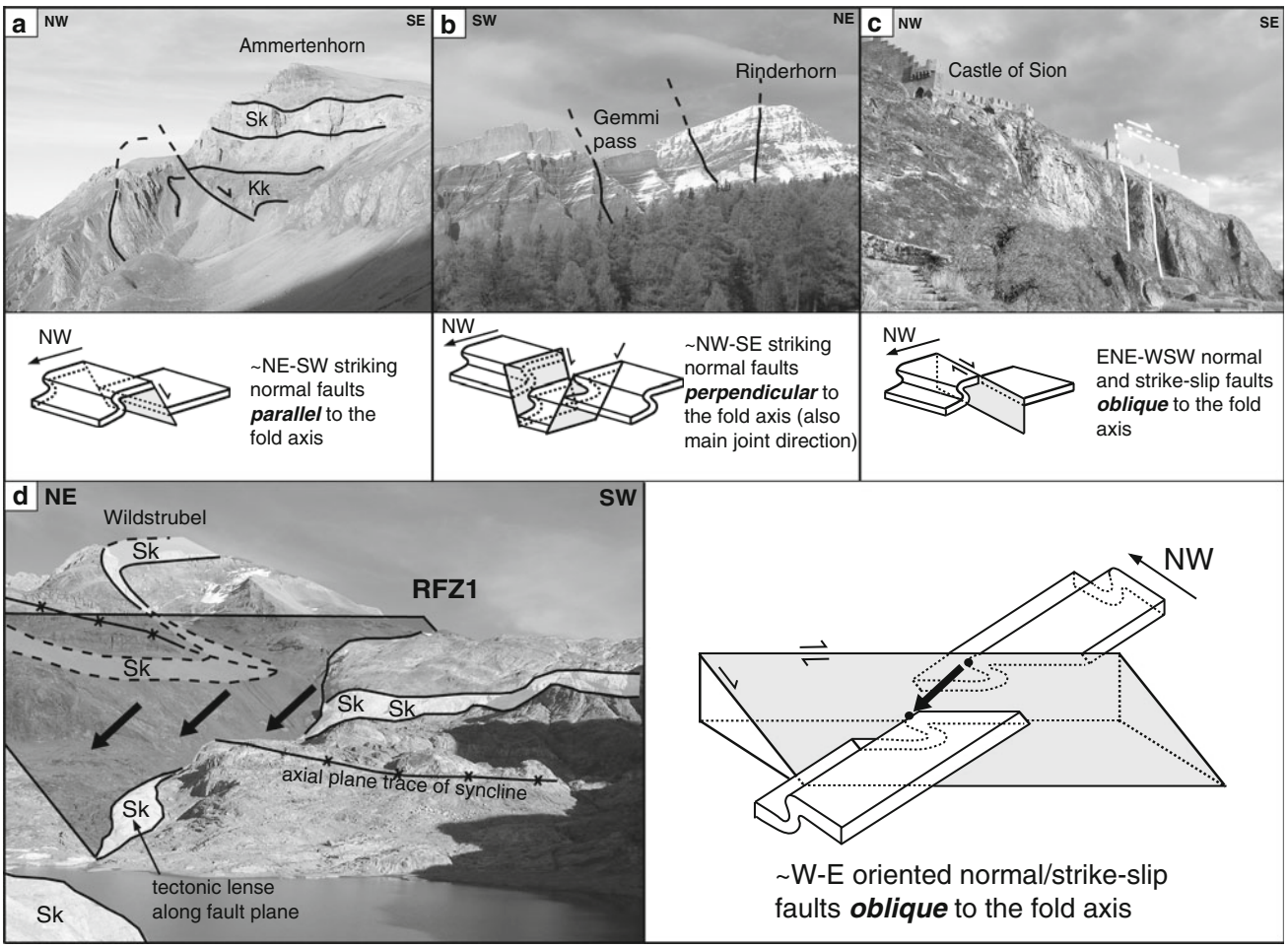

Fig. 2 Examples of the four different fault sets in the Rawil depression. All locations named on the photographs are indicated in Fig. 1b. **a** Fault set 1: NE-SW striking normal fault developed on the normal limb of a NW verging anticline in the frontal part of the Wildhorn nappe. **b** Fault set 2: NE-SW striking normal faults and mega-joints in the Gemmi pass area (e.g. Ustaszewski et al. 2007). **c** Fault set 3: ENE-WSW striking vertical strike-slip faults close to Sion in the Rhone Valley. **d** Fault set 4: WNW-ESE striking fault in the frontal part of the Wildhorn nappe, which is one of the two faults described in this study (RFZ1). The RFZ1 cuts through already folded sedimentary protoliths such as limestones, marls and sandstones. Slickensides on fault planes point to an oblique slip vector with SSW-side-down and dextral sense of movement (*black arrows*). The RFZ1 offsets the fold axis of a major pre-existing syncline (axial plane trace indicated on photograph), which can be used to estimate the total displacement across the fault zone (see "Estimation of displacement across the Rezli fault zones" and Fig. 5). *Sk* Schrattenkalk Formation, *Kk* Kieselkalk Formation

ENE-WSW striking, oblique-slip faults with SSE-side down and dextral sense of movement (Fig. 2c). These faults are developed all along the Rhone Valley in the southern region of the western Helvetic nappes (Pavoni 1980; Burkhard 1988a, b; Masson 1988). They are related to a wide zone of brittle deformation displacing the Penninic units on the southern side relative to the Helvetic nappes on the northern side of the valley, with dextral and south-side-down kinematics. This zone has been linked with the Simplon Fault Zone further to the south-east (Steck 1984; Burkhard 1988a, b; Mancktelow 1985, 1990, 1992; Hubbard and Mancktelow 1992; Steck and Hunziker 1994), and the combined structure is commonly referred to as the "Rhone-Simplon fault zone" or "Rhone-Simplon Line". (4) WNW-ESE striking oblique-slip faults with SSW-side down and dextral sense of movement that strike oblique to the regional fold axis trend (Fig. 2d). These faults only developed in the central part of the Wildhorn nappe. Burkhard (1988b) and Huggenberger and Aebli (1989) assumed that they developed above a similarly oriented dextral shear zone in the underlying crystalline basement, which offsets the Aiguilles Rouge and Mont Blanc massifs relative to the Gastern and Aar massifs. The Rezli fault zones, described further below, belong to this set of oblique faults.

The Rezli fault zones (RFZ)

The RFZ are two parallel fault zones (a northern RFZ1 and a southern RFZ2) with similar orientation and sense of

displacement belonging to fault set 4 displayed in red on Fig. 1b. They are exceptionally well exposed over a length of ~2 km in the central part of the Wildhorn nappe in a recently deglaciated area in front of the Rezli glacier (Figs. 2d, 3). We mapped the area on a scale of 1:5,000 (Fig. 3a) and constructed detailed profiles through each fault zone. Our results on the general structure of the area, estimates of the total displacement across the two fault zones, as well as the orientation, sense of displacement and internal architecture of the fault zones are summarized in the following sections.

Stratigraphy and structure of the host rocks cut by the RFZ

The RFZ cut straight through previously folded and faulted sedimentary rocks of the Wildhorn nappe. In the mapped area, these rocks include interbedded marls and limestones of the Cretaceous Kieselkalk, Drusberg and Seewen Formations, massive limestones of the Cretaceous Schrattenkalk Formation and sandstones of the Cretaceous Garschella and Tertiary Klimsenhorn and Wildstrubel Formations. A stratigraphic profile is given in Fig. 3b, together with a short description of the rock types in the figure caption. More detailed descriptions of the stratigraphy can be found in Schaub (1936), Furrer (1938), and Föllmi and Gainon (2008). For convenience and conciseness, we follow Furrer (1956) in distinguishing two informal mappable members of the Seewen Formation, the lower dominantly calcareous "Seewerkalk" and the upper marly "Seewerschiefer".

In the mapped area, the Cretaceous and Tertiary rocks are folded into a large-scale syncline, which is part of a series of anticlines and synclines present in the frontal part of the Wildhorn nappe (Figs. 2d, 3c). Fold axes of abundant centimetre- to metre-scale folds associated with this syncline trend NE-SW to E-W and mainly plunge less than 20° towards the NE (Fig. 4a). Two cleavage generations are observed. A penetrative slaty cleavage (S_1) dips 10–40° toward SE and is well developed in the Kieselkalk Formation, the Drusberg Formation, the Seewerschiefer member, and the Wildstrubel Formation (Fig. 4a). This first cleavage is generally axial plane to regional F_1 folds. However, a younger spaced cleavage (S_2) typically dips slightly steeper than S_1 to the SE and is locally strongly developed, especially in the Kieselkalk Formation. Rarely (e.g. at Swiss coordinates 605178/138465), a subsequent and distinctly differently oriented crenulation cleavage (S_3 on Fig. 4a) is developed in the Seewerschiefer member, transverse to the general trend of regional F_1 folds.

The normal limb of the large-scale syncline is displaced by three thrusts T1–T3 with offsets of up to several tens of metres (Fig. 3a, c). T1 and T2 dip 40–50° towards the SE with a few measurements indicating that they are slightly steeper oriented than the axial plane foliation (S_1) of the large-scale syncline (Fig. 4a).

Several sets of veins cross-cut all units in the mapped area. The composition of these veins generally reflects the host rock, i.e. dominantly calcite veins but with common quartz veins in the Eocene sandstones. The most prominent and abundant veins are extensional and filled with blocky calcite and quartz. They typically strike NW-SE, with a steep to moderate dip toward SW or NE (Figs. 4b, 7a). This orientation corresponds to that of fault set 2 (Figs. 1b, 2b). These straight veins locally bisect conjugate sets of brittle-ductile shear zones outlined by en-echelon, sometimes sigmoidal, vein sets. The overall geometry indicates synchronous and relatively late NW-SE shortening and NE-SW extension. Such extensional veins occur throughout the Helvetic nappes in western Switzerland and reflect NE-SW-directed fold-axis parallel extension overprinting earlier top-to-NW-directed shear (Dietrich 1989a; Ramsay 1989).

Besides the two Rezli fault zones described in detail below, a large number of smaller brittle faults cross-cut the mapped area (Fig. 4c). Most of them are developed in the Eocene Klimsenhorn and Wildstrubel Formations. Especially the bands of Klimsenhorn sandstone are regularly offset by such smaller-scale faults (Fig. 3a). Most of them dip 40–60° toward SW and show a SW-side-down sense of movement (Fig. 4c). A few strike-slip faults with both sinistral and dextral offsets are present.

Estimation of displacement across the Rezli fault zones

The general orientation and sense of displacement across the two Rezli fault zones can be directly established from field observations, although the number of measurable slickensides on fault planes is unfortunately rather small (Fig. 4d, e). Sharp fault planes exposed in both fault zones mainly dip 30–60° towards the SW-SSW, with exception of the eastern part of RFZ1 that dips more towards the W. Slickensides present on the fault planes indicate a SW-side-down sense of movement with a variable dextral component (Fig. 4d, e; for details see "Geometry and internal architecture of the northern Rezli fault zone (RFZ1)", "Geometry and internal architecture of the southern Rezli fault zone (RFZ2)" below). Estimation of total displacement across the fault zones is not straightforward. Since the RFZ cut through already folded and faulted sediments, an estimation of total displacement relies on the correct correlation of structures or units on both sides of the fault zones. This is difficult insofar as (1) the original thicknesses of sedimentary units in the area already varied prior to faulting and (2) structures developed prior to faulting are not perfectly cylindrical. The total 3D displacement across a fault can only be determined directly from corresponding

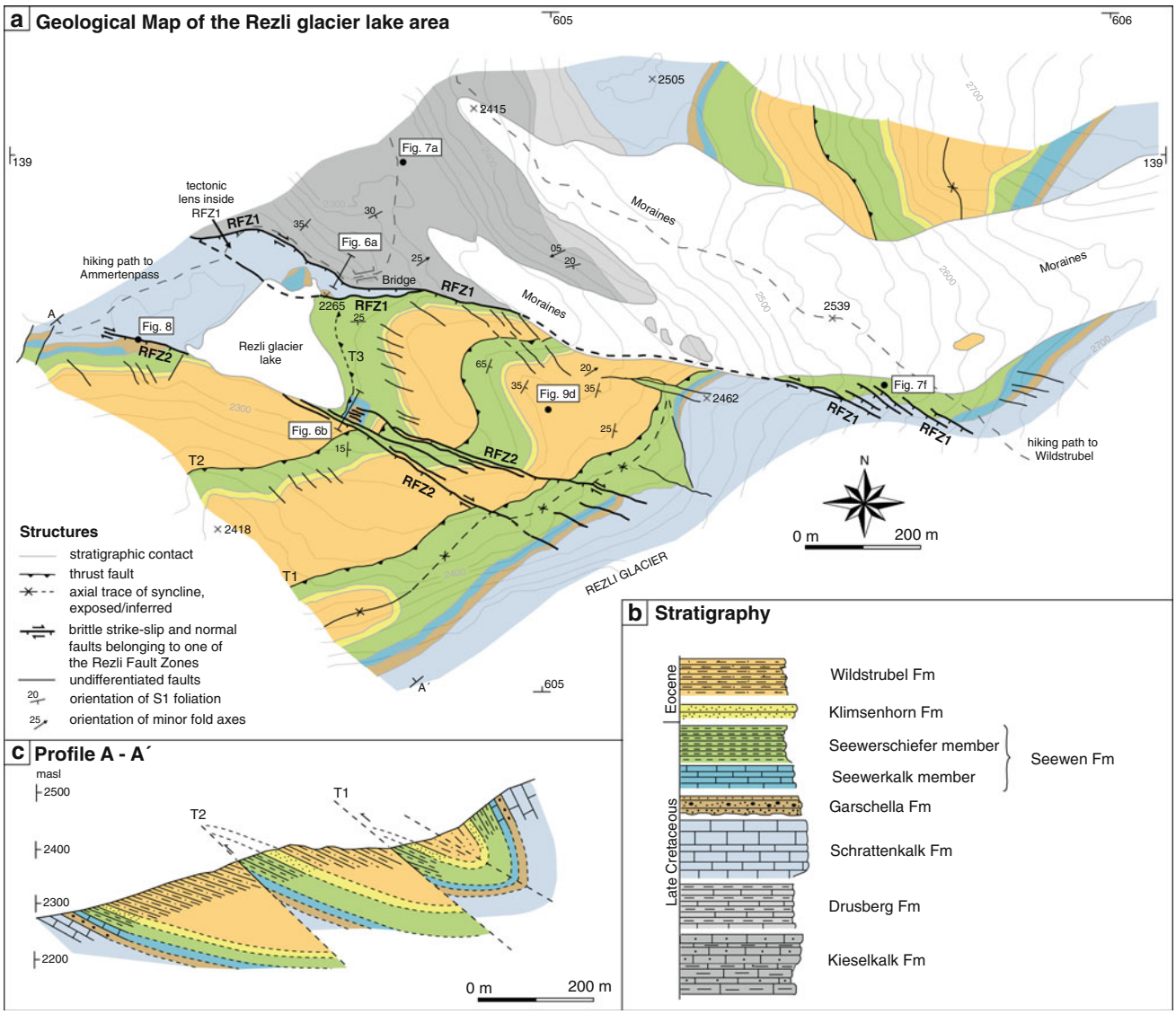

Fig. 3 **a** Geological map of the Rezli fault zones (RFZ). Location of the map is indicated on Fig. 1b. **b** Stratigraphic column of the study area. The following units have been mapped: (1) Kieselkalk Fm (Hauterivian): dark-grey, brownish alternation of marls and crinoidal, siliceous limestones, (2) Tierwis Fm (Barremian), Drusberg member: bedded grey marls and marly, siliceous limestones, (3) Schrattenkalk Fm (Late Barremian to Early Aptian, "Urgonian"): massive, light-grey, bioclastic and oolitic limestone rich in rudists and corals, unconformably overlain by (4) Garschella Fm (late Aptian-middle Turonian): glauconitic and fossil-rich sandstones and limestones with abundant phosphate nodules, (5) Seewen Fm (late Turonian-Campanian): pelagic, micritic, light-grey limestones (biomicrite), rich in pyrite (Seewerkalk member) and yellowish, bioturbated marls also rich in pyrite (Seewerschiefer member), unconformably overlain by (6) Klimsenhorn Fm (Lutetian-Bartonian): massive, yellowish quartz-sandstone with layers of dark-grey, fossil-rich limestones, (7) Wildstrubel Fm (Bartonian-Priabonian): dark-brownish, sandy, mica-rich marls and sandstones. **c** Geological profile through the mapped area. The profile trace is indicated on **a**. The profile shows the geometry of the area as it existed before the RFZ developed: the sedimentary rocks of the Wildhorn nappe are folded into a large-scale syncline with thrusts developed on the normal limb of the syncline

piercing points of a linear feature (e.g. a fold axis) intersecting the planar surface. If the displacement direction can be estimated from slickenside measurements, then the displacement of planar surfaces (e.g. lithological boundaries) can give sufficient constraint. However, in this case it must be assumed that the movement direction remained the same throughout the fault history.

In order to estimate the total offset, Burkhard (1986) constructed two regional schematic cross-sections on both sides of the RFZ (his Fig. 4). He considered three regional fold axes to establish piercing points: (1) the major frontal anticline exposed NW of our area and passing through the Flueseeli, (2) the syncline passing through our study area (Figs. 2d, 3), and (3) the adjacent anticline following to the SE. From his Fig. 4, the offset of (1) is ca. 1,200 m horizontally and 700 m vertically, whereas (2) and (3) give lower values of around 250–300 m horizontally and 200 m vertically. This is consistent with the observation that the

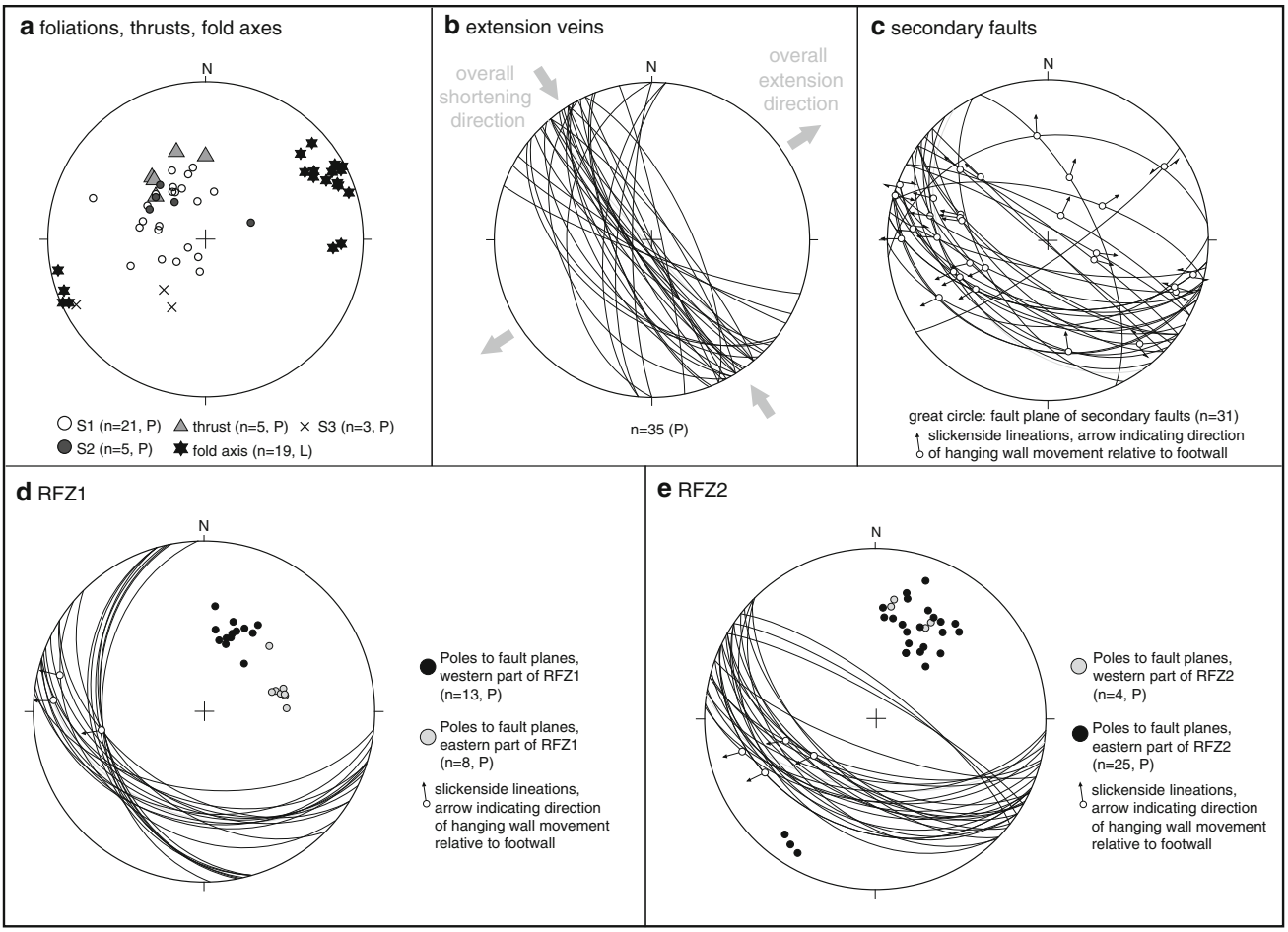

Fig. 4 **a** Stereoplot of the first axial plane foliation S1, the locally developed crenulation cleavages S2 and S3, thrust surfaces and fold axes from the study area. **b** Stereoplot of extension veins. **c** Stereoplot of fault planes and slickensides from secondary faults throughout the study area. **d** Stereoplot of fault planes and slickensides from the RFZ1. **e** Stereoplot of fault planes and slickensides from the RFZ2. Lower hemisphere equal area projections, computed with Stereonett software of Rick Allmendinger and TectonicsFP Software

RFZ appear to be losing displacement to the ESE, where RFZ1 in particular becomes segmented (Fig. 3a; see "Geometry and internal architecture of the northern Rezli fault zone (RFZ1)" below).

We repeated this analysis on the more local scale of our detailed map area (Fig. 5). We constructed three vertical profiles parallel to the strike of the mean orientation of RFZ1 and RFZ2 and used the Eocene Klimsenhorn Formation as a marker horizon. The profiles allow a first-order approximation of the offset, but the exact values depend on (a) assumptions on the shape of the syncline in all profiles and (b) assumptions on the offset of the Klimsenhorn Formation across thrust T1 on profile 2 and 3. Assuming a cylindrical shape of the syncline and a conservative offset across T1, the total displacement across the two fault zones RFZ1 and RFZ2 can be estimated: Between profile 1 and 2, respectively, located north and south of the RFZ1 (Fig. 5a), the synclinal hinge of the Klimsenhorn Formation is offset by ~150 m vertically (S-side down) and ~500 m horizontally (dextral; Fig. 5b). Between profile 2 and 3, respectively, located north and south of the RFZ2 (Fig. 5a), the synclinal hinge is offset by ~50 m vertically (S-side down) and ~180 m horizontally (dextral; Fig. 5b). Considering the uncertainties involved in profile construction, the value of ~200 m for the combined vertical offset across the RFZ corresponds very well to that estimated by Burkhard (1986). However, the dextral horizontal offset of ~680 m is somewhat larger, reflecting our interpretation of faults T1–T3 as thrusts rather than normal faults, as in Burkhards Fig. 4. The value is still less than the ~1,200 m horizontal displacement he estimated across the RFZ from the offset of the frontal anticline just to the NW of the map of Fig. 3a. In summary, the total displacement across the RFZ in our study area is on the order of ~200 m vertically (S-side down) and ~680 m horizontally (dextral), with more displacement across RFZ1 than across RFZ2.

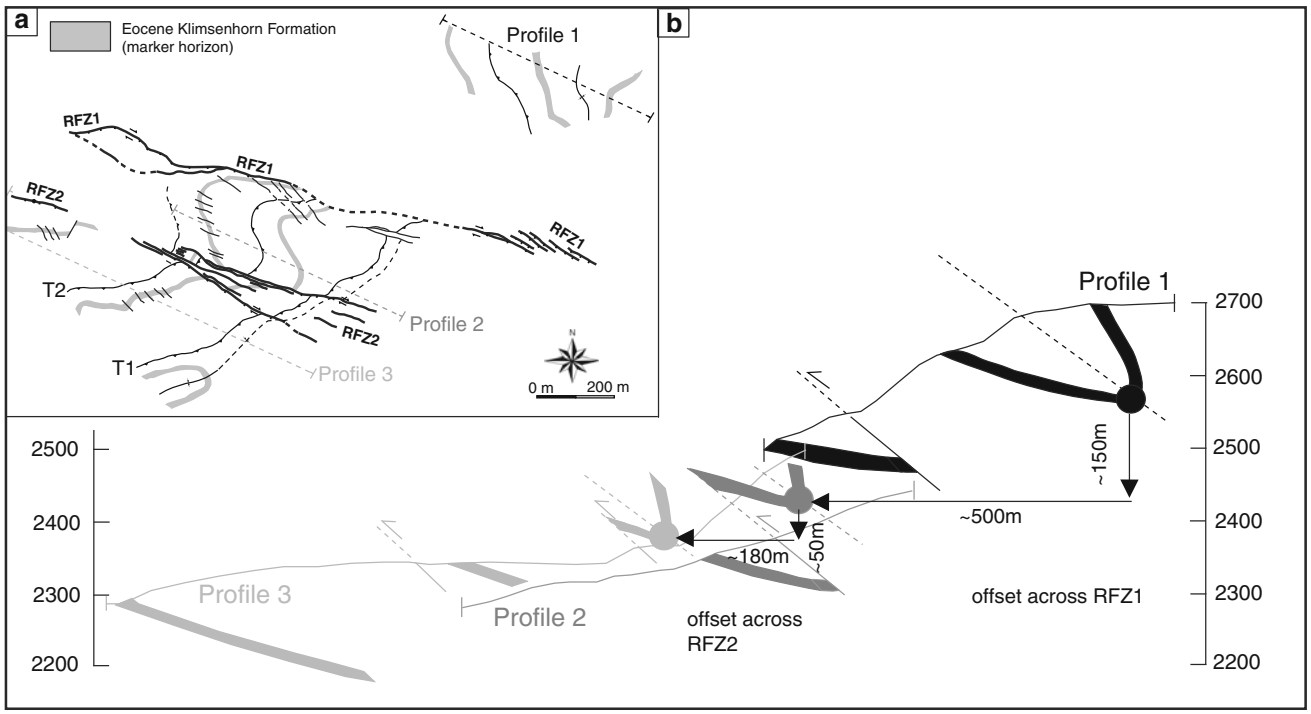

Fig. 5 **a** Simplified sketch of the tectonic situation in our study area, derived from Fig. 3a, with only the RFZ and the Eocene Klimsenhorn Formation indicated. **b** Three superimposed cross-sections through the study area. Profile 1 is located to the north of RZF1, profile 2 is located between RFZ1 and RFZ2, and profile 3 is located to the south of RZF2. The three profiles allow a first-order approximation of the total displacement across the fault zones with the help of the large-scale syncline exposed in the study area (Fig. 2d) by correlating constructed fold hinges of the Eocene Klimsenhorn Fm on either side of the fault zones

Geometry and internal architecture of the northern Rezli fault zone (RFZ1)

The northern fault zone in the mapped area (RFZ1) is exposed in two parts: a western part and an eastern part separated by an unexposed area covered by moraines (Figs. 2d, 3a). The western part consists of (a) a main fault branch separating the Kieselkalk Formation in the footwall from the Schrattenkalk Formation and Seewerschiefer member in the hanging wall and (b) a smaller subordinate branch separating the Schrattenkalk Formation in the footwall from the Seewerschiefer member in the hanging wall. The subordinate branch merges with the main branch below and above the Rezli glacier lake—the block of Schrattenkalk Formation captured between the main and subordinate branches forms a tectonic lens ~200 m long and several tens of metres wide inside the RFZ1 (Figs. 2d, 3a).

The internal geometry of the main branch of the western part of RFZ1 is complex. A detailed profile across it is given in Fig. 6a. In the Kieselkalk Formation forming the footwall, a 2–10 m wide damage zone is developed, with increasing density of anastomosing shear planes, small-scale folds and fractured lenses towards the contact with the Schrattenkalk Formation in the hanging wall. Bedding planes, foliation planes and extensional veins from the Kieselkalk Formation are incorporated into this damage zone (Figs. 6a, 7b).

The contact between the Kieselkalk and Schrattenkalk Formations is mostly formed by sharp, through-going fault planes. Some of these fault planes can be followed for several tens of metres and are generally very straight (Figs. 6a, 7c, d). The fault planes have a mean orientation of 201/41 (dip direction/dip; Fig. 4d). Slickensides are only very rarely preserved but, where present, indicate a SW-side-down movement with a minor dextral component (Fig. 4d). Locally, lenses of Schrattenkalk Formation are found below these sharp fault planes (Figs. 6a, 7c), indicating that the juxtaposition of Kieselkalk and Schrattenkalk Formations took place before the formation of the sharp fault planes.

In the Schrattenkalk Formation forming the hanging wall, the sharp fault planes are locally marked by a mm- to cm-thick, yellowish, cemented fault gouge. In addition, the fault planes are bordered by mm- to cm-thick layers of cataclasites (Fig. 7d). These cataclasites consist of rounded µm- to mm-sized clasts derived from Schrattenkalk limestones and veins in a fine-grained matrix cross-cut by several generations of veins and stylolites (Fig. 7e). The cataclasites are separated from the host rock by thick, dark

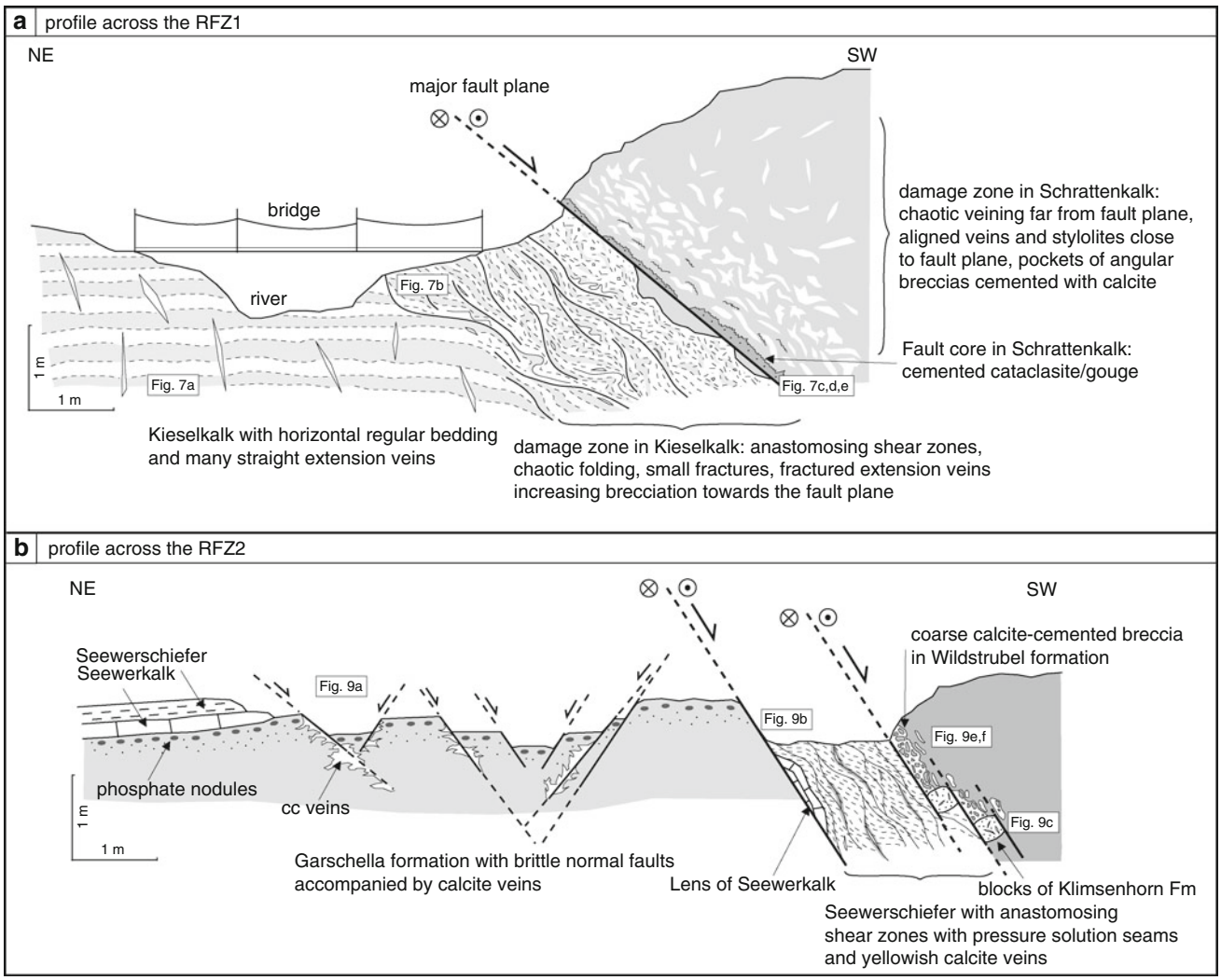

Fig. 6 **a** Profile across the northern Rezli fault zone (RFZ1). **b** Profile across the southern Rezli fault zone (RFZ2). The locations of the profiles are indicated on Fig. 3a

stylolites (Fig. 7d). Moving away from the fault planes and cataclasites into the hanging wall, abundant parallel veins and stylolites occur in the Schrattenkalk Formation over a distance of 10–20 cm, with a transition into more indistinct, randomly oriented, irregular veins occurring up to 5–10 m away from the fault planes (Fig. 6a).

The eastern part of the RFZ1 above the moraine-covered area separates the Seewerschiefer member in the footwall from the Schrattenkalk Formation in the hanging wall (Fig. 3a). In the Seewerschiefer member, anastomosing shear zones and pressure solution seams accompany the fault planes, whereas in the Schrattenkalk Formation forming the hanging wall, the fault planes are coated with 1–5 cm thick, white to yellowish, coarse calcite crystals (Fig. 7f).

In this eastern area, the main fault zone from the western part of the RFZ1 becomes segmented and several smaller parallel fault zones are present. Each of these smaller fault zones consists of one sharp main fault plane with smaller conjugate faults that merge into the main fault plane (Fig. 7f). The orientation of these smaller fault planes is slightly different from the orientation of the main fault plane in the western part. They have a mean orientation of 254/40 (dip direction/dip; Fig. 4d), with their strike direction rotated in a clockwise sense relative to the main fault zone in the western part. Slickensides on the fault planes indicate a dominantly normal, W-side-down sense of movement. The total amount of displacement across the multiple fault zones also seems to be smaller than across the main fault zone in the western part (cf. Fig. 6a). The segmentation, rotation of fault strike, and decrease in total displacement toward the east are all typical features observed at the termination of strike-slip fault zones. Such a structure was referred to as a “horsetail splay” by

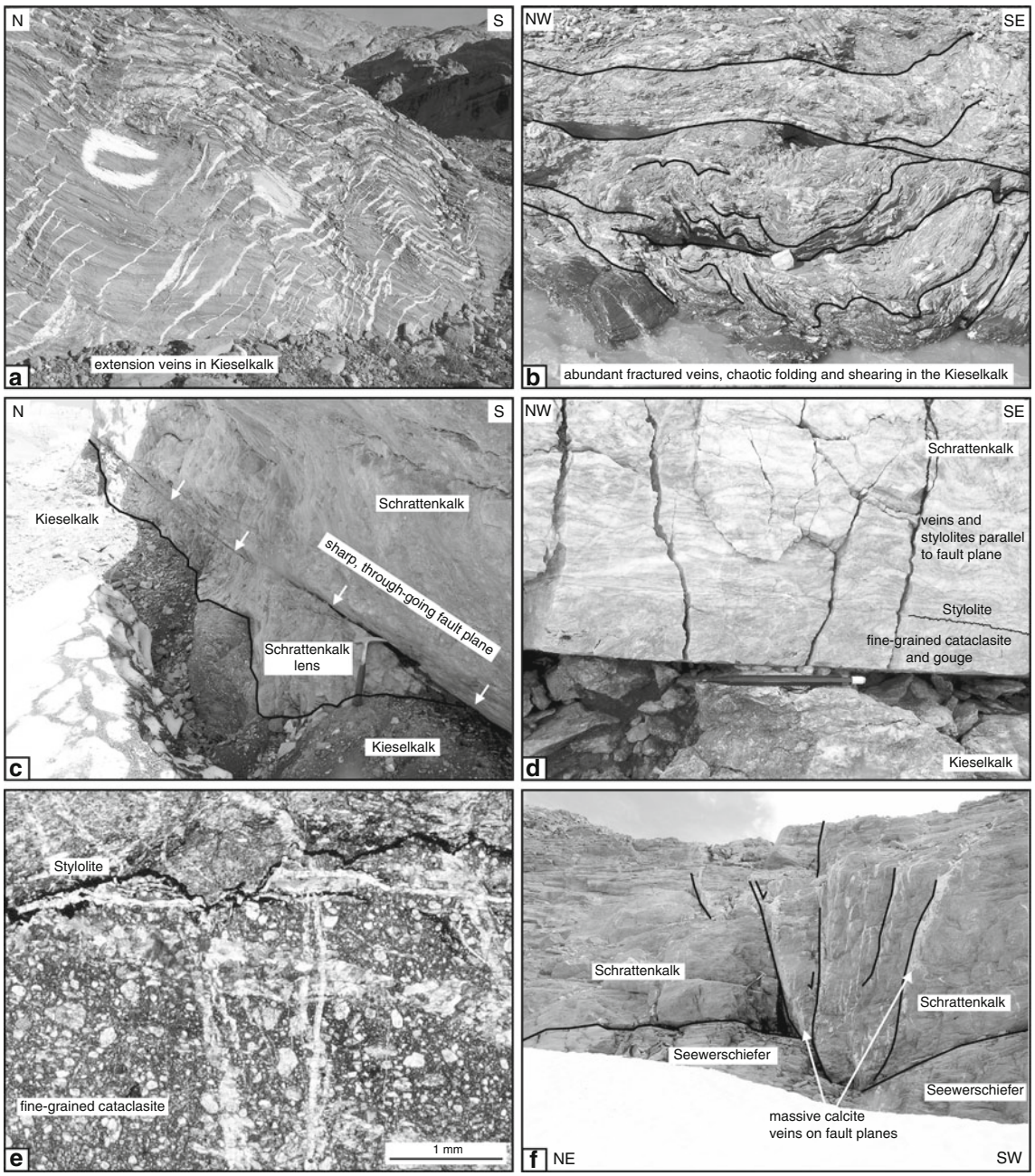

Fig. 7 **a**–**e** Field photographs from RFZ1. The locations of the photographs are indicated on Figs. 3 and 6. **a** Straight extension veins in Kieselkalk Fm. Size of hiking path sign in the foreground (white rectangle) ~30 cm. **b** Damage zone of RZF1 in the Kieselkalk Formation. Anastomosing shear zones, fractures and chaotic folds are developed. The straight extension veins present outside the damage zone in the Kieselkalk Fm are fractured and incorporated into the damage zone. Width of view ~1 m. **c** The RFZ1 separating Kieselkalk Fm in the footwall from Schrattenkalk Fm in the hanging wall. A tectonic lens of Schrattenkalk Fm is present below the major, through-going, sharp fault plane. Hammer in the foreground for scale. **d** Close-up of main fault plane of RFZ1. In the Schrattenkalk Fm, the main fault plane is accompanied by fine-grained cataclasite and gouge. Stylolites and sheared veins are present in the damage zone of the Schrattenkalk Fm. Pencil for scale. **e** Thin section photograph of a fine-grained cataclasite derived from the Schrattenkalk Fm cross-cut by a stylolite and several generations of veins. **f** One of the fault planes of the eastern part of the RFZ1. The fault plane displaces the Seewerschiefer member in the footwall against the Schrattenkalk Fm in the hanging wall by ~1 m. The fault plane is coated with thick calcite and accompanied by minor conjugate faults. Hammer in the centre for scale

Christie-Blick and Biddle (1985) or as a "trailing extensional imbricate fan" by Woodcock and Fischer (1986).

Geometry and internal architecture of the southern Rezli fault zone (RFZ2)

The southern fault zone in the mapped area (RFZ2) is also exposed in two parts: a western part below the Rezli glacier lake and an eastern part above the lake (Fig. 3a). The western part juxtaposes the Schrattenkalk Formation in the footwall against the Garschella Formation and the Seewerschiefer member in the hanging wall (Figs. 3a, 8). The fault zone developed here consists of a single sharp through-going fault plane with a mean orientation of 200/52 (dip direction/dip; Fig. 4e). This fault plane is accompanied on both sides by a fine-grained cemented cataclasite and cemented fault gouge up to 20 cm wide, probably derived from limestones of the Schrattenkalk Formation. In the Schrattenkalk Formation forming the footwall, a 1–2 m wide zone with irregular pockets of coarse-grained cataclasite, cross-cut by multiple sets of veins occur. These pockets gradually pass into areas where the Schrattenkalk Formation is not brecciated, but cross-cut by many rather indistinct, irregular calcite veins (Fig. 8). In the Garschella Formation forming the hanging wall, sharp brittle faults and calcite veins occur adjacent to the fine-grained cataclasites.

The eastern part of RFZ2 above the Rezli glacier lake has a much more complex internal structure (Fig. 6b). It cuts through the Garschella Formation, the Seewen Formation, the Klimsenhorn Formation and the Wildstrubel Formation, with each formation present both in the hanging and footwall (Fig. 3a). The fault zone consists of several smaller parallel straight and sharp fault planes that have a mean orientation of 207/52 (dip direction/dip; Fig. 4e). Only a few slickensides on the main fault planes were observed and they indicate a SW-side-down sense of movement with a dextral component (Fig. 4e).

The fault rocks and the characteristics of the damage zone within which the sharp fault planes developed differ depending on the lithology they transect. Figure 6b shows a profile across the RFZ2 just above the lake. In the Garschella Formation, conjugate sets of discrete normal faults are developed. They can be easily recognised because they offset a marker layer of dark phosphate nodules present in the Garschella Formation, with displacements of 50 cm to 1 m (Figs. 6b, 9a). These fault planes are accompanied by irregular white calcite veins that propagate outwards from the fault planes for a few centimetres. Except for these veins associated with the smaller fault planes, no real damage zone is developed in the Garschella Formation close to the major fault planes and the sandstones remain intact and effectively undeformed.

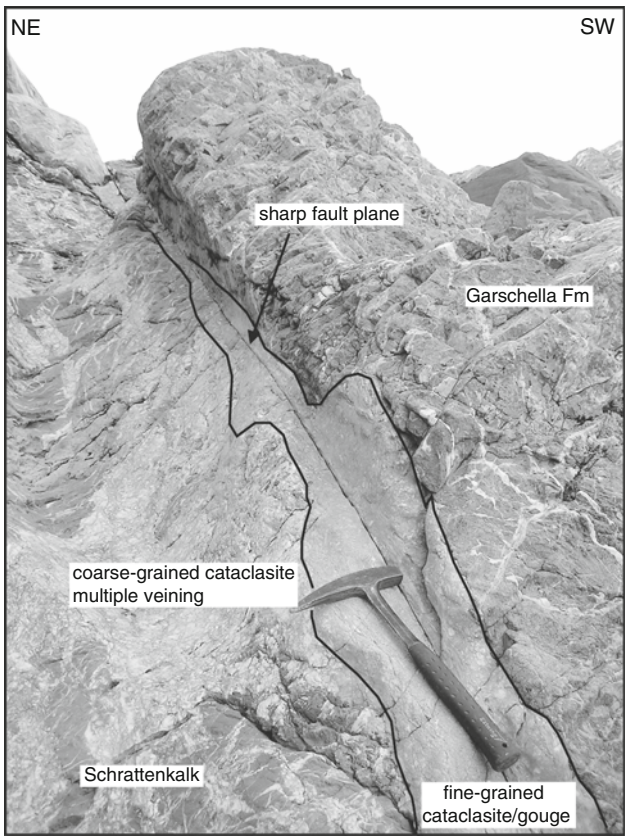

Fig. 8 Field photograph from the western part of the RFZ2 below the Rezli glacier lake. The location of the photograph is indicated on Fig. 3. The fault juxtaposes the Schrattenkalk Fm in the footwall against the Garschella Fm in the hanging wall. A sharp through-going fault plane is accompanied by fine-grained cataclasite and angular breccia in the Schrattenkalk Fm. Hammer for scale

The Seewen Formation behaves in a more ductile manner. Isolated elongated lenses of boudinaged Seewerkalk member occur within a marly matrix derived from the Seewerschiefer member adjacent to sharp, through-going fault planes (Figs. 6b, 9b). The marls are cross-cut by a network of anastomosing shear zones. These shear zones partly developed along yellowish calcite veins and are often surrounded by dark pressure solution seams (Fig. 9b). Such shear zone networks, which are up to several tens of metres wide, occur in the Seewerschiefer member with decreasing intensity away from the sharp fault planes.

In contrast, the sandstones and sandy marls of the Klimsenhorn and Wildstrubel Formations behave similarly to the Garschella Formation. Angular blocks of Klimsenhorn sandstone, full of brittle, randomly oriented, white calcite and quartz veins, occur in a matrix of Seewen marls adjacent to major fault planes (Fig. 9c). In the Wildstrubel Formation, 10–50 cm wide coarse breccias are developed close to major fault planes. These breccias contain angular as well as rounded clasts (up to several cm in size) that are

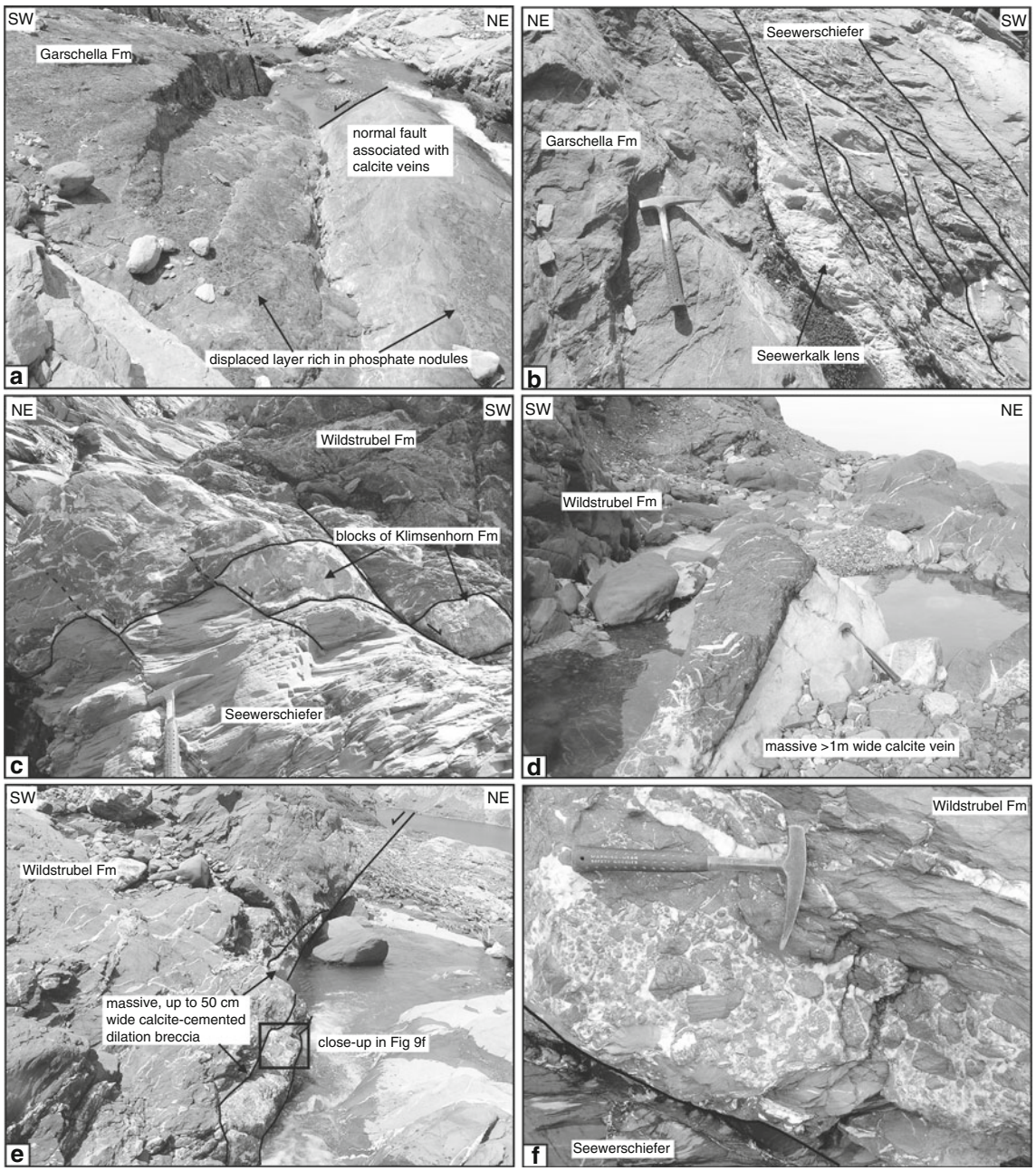

Fig. 9 Field photographs from the eastern part of the RFZ2 above the Rezli glacier lake. The locations of the photographs are indicated on Figs. 3 and 6. **a** Conjugate brittle normal faults displace a layer rich in phosphate nodules in the Garschella Fm. Width of view ~10 m. **b** Tectonic lens of Seewen limestone adjacent to the main fault plane. Many anastomosing shear zones developed in the Seewen marls. Hammer for scale. **c** Angular blocks of Klimsenhorn Fm incorporated into the fault zone. Hammer for scale. **d** Massive, up to 1 m wide calcite veins in the Wildstrubel Fm. Hammer for scale. **e** Main fault plane associated with coarse angular breccia in the Wildstrubel Fm. Width of view ~10 m. **f** Close-up from **e**. Breccia of angular to rounded clasts of Wildstrubel Fm cemented by blocky, white calcite. Hammer for scale

cemented by yellowish crystalline blocky calcite (Fig. 9e, f). Away from the fault planes, the Wildstrubel Formation is characterised by abundant veins up to 1 m wide, filled with coarse, crystalline, yellowish calcite (Fig. 9d). In addition, smaller sharp brittle fault planes cross-cut the Wildstrubel Formation.

Discussion

Oblique-slip movement on the RFZ

The RFZ are shallow- to moderately dipping (ca. 30°–60°) fault zones with an oblique-slip displacement vector. They

must have formed in almost this same orientation, because the local orientation of the fold axes corresponds to the regional one, as does the generally vertical orientation of extensional joints and veins associated with fault set 2. The RFZ are part of fault set 4 in the Rawil depression, which typically have a WNW-ESE strike transverse to the regional fold trend and an oblique-normal (dextral plus SSW-side-down) sense of movement. Oblique-slip is not in accord with the simple Andersonian theory for normal, thrust and strike-slip faults (Anderson 1951) but is not uncommon in nature, particularly in zones of transtension (e.g. Ballance and Reading 1980; Huerta and Rodgers 1996; Ferraccioli and Bozzo 2003; Henry et al. 2007). Oblique-slip faulting is also produced in analogue sandbox experiments of transtensional pull-apart basins (Basile and Brun 1999; Wu et al. 2009). As summarized by Price (1966, p. 79–83), oblique-slip faults could reflect (1) tilting subsequent to faulting, (2) a stress field with principal axes inclined to the vertical and horizontal in an isotropic material (Williams 1958), (3) rotation of principal stress axes in an anisotropic material (e.g. Cobbold 1976; Kocher and Mancktelow 2006), (4) failure along a plane of anisotropy or plane of weakness, or (5) reactivation of movement along a pre-existing fault plane. For the case of movement on a pre-existing surface, slip should occur in the direction of maximum resolved shear stress, which will be a function of both the orientation of the plane relative to the principal stress axes and of the relative magnitudes of these principal stresses (Bott 1959). Oblique-slip faulting could also reflect (6) the imposed kinematic boundary constraints, as in transtensional pull-apart basin models (Basile and Brun 1999; Wu et al. 2009).

In the case of the RFZ, significant later tilting can be excluded and there is no evidence for precursor structures controlling the faults, which obliquely transect the folded stratigraphic sequence. The RFZ are also not refracted across lithological boundaries, in constrast to some other examples of faults that cut through sedimentary rocks with strong mechanical contrasts between different layers (e.g. Schöpfer et al. 2007). Transtensive, oblique-normal slip on the RFZ (and fault set 4 in general) is probably determined by their location within the footwall of the Rhone-Simplon fault zone, which imposes an oblique-slip dextral and normal boundary condition to the south along the Rhone Valley.

Internal fault zone architecture of the RFZ

Characterizing the internal architecture of fault zones and their evolution through time is of great importance for understanding the general mechanical behaviour of the upper crust (e.g. earthquakes) and the migration of fluids through it (hydrocarbons and water). Field, experimental and numerical modelling studies over the last decades aimed to better establish the mechanical, seismological and hydrological behaviour of such fault zones (e.g. Kurz et al. 2008; Wibberley et al. 2008 and references therein). Conceptual models describing the internal architecture of fault zones generally distinguish two parts: (1) the fault core and (2) the adjacent damage zone (e.g. Caine et al. 1996; Braathen et al. 2009). The fault core is defined as that part where most of the displacement occurred, whereas the damage zone comprises the network of subsidiary structures surrounding the fault core. Elements that can build up both fault core and damage zone include single fractures and slip-planes, tectonic lenses of wall rock, and a whole range of fault rocks derived from variably deformed protolith (e.g. Caine et al. 1996; Braathen et al. 2009).

Field studies of internal fault zone architecture have demonstrated that natural fault zones usually show a very complex arrangement of fault core and damage zone elements both in 2D and 3D and that the arrangement of these elements varies through time during the evolution of a fault zone (e.g. Kelly et al. 1998; Faulkner et al. 2003; Bonson et al. 2007; Wibberley et al. 2008). Several factors controlling the arrangement of fault zone elements have been proposed (e.g. Wibberley et al. 2008): (1) the geometry of pre-existing structures and heterogenities (bedding, foliation, other faults and folds), (2) the stress regime in which faulting occurred (normal vs strike-slip vs thrust faulting), (3) the depth of faulting (pT conditions), (4) the total amount of displacement that occurred across the fault and (5) the rock types involved (e.g. sedimentary vs. crystalline, consolidated vs. weakly consolidated sediments).

The Rezli fault zones developed in pre-structured host rocks, in which folds, foliations, thrusts and minor faults were already present. They formed in a stress regime that produced oblique-slip faulting, with normal and dextral components. The depth of faulting is only loosely constrained. The host rocks of the RFZ belong to the frontal part of the Wildhorn nappe, which experienced a diagenetic overprint of $<\sim 240$°C and 2–3 kbar (Burkhard 1988a, 1988b; Frey and Mählmann 1999), which corresponds to a depth of ~ 8 km. Faulting therefore occurred at $\leq \sim 8$ km depth. The total amount of displacement across the RFZ lies in the range of a few hundred metres. The factor that varies most across and along the RFZ is the lithology. Massive limestones, bedded marls and limestones, marls and sandstones are incorporated into the fault zones. This variation in rock type exerts the main control on the internal fault zone architecture of the RFZ.

A schematic illustration of our observations made along the RFZ depending on the lithology in which the faults developed is given in Fig. 10. A common element in all rock types are sharp, planar fault planes that cross-cut all previous structures and that therefore developed relatively

late in the faulting history (Figs. 7c, d, 8). Whether these fault planes formed during seismic slip events or not cannot be inferred from field observations alone (e.g. Cowan 1999). Since they often separate different lithologies (Fig. 7c, d) and accommodate a significant part of the total displacement, we consider them as fault cores. However, how much of the total displacement occurred specifically on the distinctive sharp fault planes and how much of the total displacement is distributed in the adjacent damage zones cannot be accurately estimated. Apart from the sharp fault planes common to all lithologies, the different rock types have responded very differently to deformation along the RFZ, as summarized below.

In the massive limestone (Fig. 10a), fault gouge and fine-grained cataclasites form the fault core. Tectonic lenses of limestones (of cm- up to several tens of metres in size) surrounded by major fault planes probably formed as the result of asperity bifurcation (Childs et al. 1996). The surrounding damage zone consists of a network of veins and stylolites increasing in intensity toward the fault core, with coarse-grained cataclasites cross-cut by multiple sets of veins occurring in pockets. The presence of stylolites (as the locus of material solution) and veins/cemented breccias (as the locus of material deposition) point to important pressure solution and material flux on a mm- to m-scale inside the fault damage zone. According to Willemse et al. (1997), such pressure solution seams and veins play an important role in fault zone nucleation in limestones. Similar features were reported by Hausegger et al. (2009) from a large-scale strike-slip fault (offset on the order of 2–3 km) that cuts through limestones. According to their observations, deformation started with the formation of shear fractures, stylolites and veins, followed by more intense brecciation of the host rock, until shearing was concentrated in the cataclasite and on the fault planes, indicating that the fault zone became narrower through time. Certainly the latest movements in the RFZ occurred on very narrow, discrete surfaces (Figs. 7c, d, 8), reflecting late and strong localization within a very narrow zone (often on the mm-scale, or less, in width).

In bedded marls and limestones (Fig. 10b), the fault planes are directly adjacent to an up to 10 m wide damage zone where anastomosing shear zones, brittle fractures and chaotic folds occur. In contrast to the more massive limestones described above, no new veins formed associated with the damage zone in this lithology. Deformation within this zone appears to be much "drier" than in the limestones, without preserved evidence for fluid infiltration or significant fluid-rock interaction.

Clay-rich marls (Fig. 10c) are often smeared out along the sharp fault planes over distances of several tens of metres and are cross-cut by a dense network of anastomosing shear zones and veins surrounded by dark pressure solution seams. This network extends from the fault planes into the host rock over several metres and deformation is more evenly distributed over a large area. Similar relationships have been described by Lee and Kim (2005) from

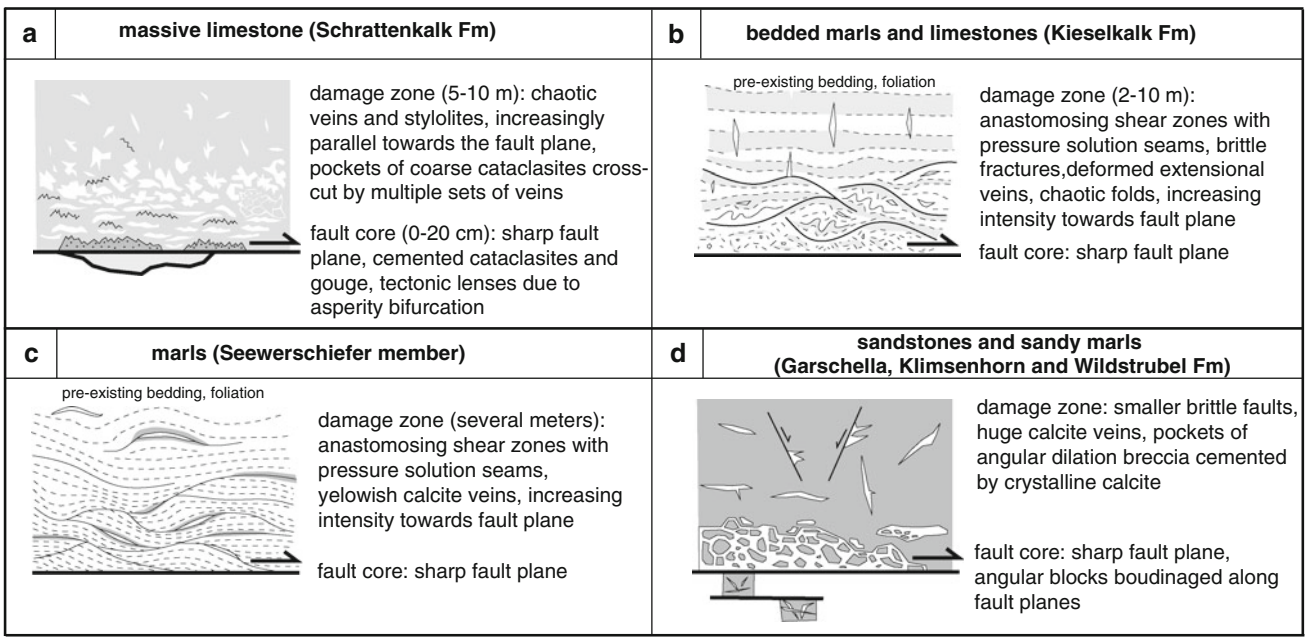

Fig. 10 Schematic sketch of fault zone elements observed in different lithologies along the RFZ: **a** massive limestone, **b** bedded marls and limestones, **c** marls, and **d** sandstones

a fault cutting through Cretaceous mudrock and by Faulkner et al. (2003) from a fault developed in phyllosilicate-rich rock.

The most striking feature in the sandstones and sandy marls (Fig. 10d) is the development of coarse, angular breccias cemented by coarse-grained calcite (Fig. 9e, f). Similar breccias preferentially developed in competent lithologies were recently described by Tarasewicz et al. (2005) and Woodcock et al. (2006, 2008) from the Dent Fault in NW England. This fault cuts through a similarly layered sequence of sedimentary rocks (limestones, sandstones and mudstones) to that in the Rezli area. The authors observed that brecciation intensity depends on the lithology, with only the strongest and least permeable lithologies being brecciated. This is in accord with our observation that such breccias only occur in the strong Wildstrubel and Klimsenhorn sandstones and sandy marls. According to the scheme of Woodcock et al. (2008), the breccias along the RFZ2 may be classified as mosaic to chaotic, fragment-supported dilation breccias with a granular rather than a fibrous cement. Fluids play an important role in the formation of such breccias and mechanisms proposed include: (1) hydraulic fracturing due to an increase in fluid pressure related to, for example, a sudden decrease in permeability due to fault slip (Jebrak 1997), or (2) direct creation of cavity space due to fault slip accompanied by large amounts of fluids and high fluid pressures, in turn followed by lower fluid pressures and rapid precipitation of hydrothermal minerals such as calcite (Sibson 1986b; Tarasewicz et al. 2005). Notably, the large amount of calcite precipitated in the breccias cannot come from the sandstones/marls of the Wildstrubel Formation itself, but were probably dissolved and transported from the underlying carbonate-rich rocks such as the Schrattenkalk, Kieselkalk and Seewen Formations. Detailed isotopic analysis of the cement in this breccias and in the veins attributed to the RFZ in general could reveal more information on fluid source and veining processes, although the earlier work of Burkhard and Kerrich (1988) has already demonstrated that fluids were strongly rock-buffered in most smaller-scale faults and veins from the Helvetic nappes.

In summary, like many other fault zones, the detailed internal structure of the RFZ is very complex. In the case of the RFZ, this complexity also reflects the variety of different host rocks crosscut by the RFZ and incorporated into the fault zones. The damage zones associated with the RFZ consist of many different elements such as cataclasites, dilation breccias, stylolites, veins, brittle fractures and ductile shear zones, indicating that very different processes were active simultaneously along the same fault zone, reflecting the diversity in mechanical response of the different rock units affected.

The Neogene brittle faulting history of the Rawil depression

The Neogene, post-metamorphic, brittle faulting history of the Penninic and Austroalpine units south of the Rhone Valley has been the focus of many detailed field studies and paleostress analyses (e.g. Bistacchi and Massironi 2000; Bistacchi et al. 2000; Grosjean et al. 2004; Champagnac et al. 2004). These studies have shown that, south of the Rhone Valley, a first phase of orogen-parallel (NE-SW) extension, including normal faulting along the Simplon fault and dextral strike-slip faulting along the Rhone fault, was succeeded by a second phase of orogen-perpendicular (NW-SE) extension, the latter also recorded by the present-day stress field (Maurer et al. 1997; Delacou et al. 2004). North of the Rhone Valley, in the Helvetic nappes of the Rawil depression, the Neogene history of brittle faulting is less well constrained. This is partly due to the fact that the sedimentary rocks of the Helvetic nappes were never strongly metamorphosed. It is therefore difficult to distinguish younger faults, which developed after nappe stacking, from older syn-sedimentary faults or from faults developed during nappe emplacement. However, our detailed analysis and compilation of information from the literature has allowed us to distinguish four different fault sets in the region of the Rawil depression. The first set of faults formed during sedimentation and was reactivated during nappe stacking. The other three fault sets formed after emplacement of the Helvetic nappes and were therefore active during the Neogene.

Cross-cutting relationships do not reveal a clear picture of the relative age of the three Neogene brittle fault sets. The faults of set 2 were commonly assumed to be the youngest brittle structures in the Rawil depression (e.g. Dietrich et al. 1983; Dietrich 1989a; Ramsay 1989). One of these faults has even been active in post-glacial times (Ustaszewski et al. 2007). However, the Rezli fault zones, which belong to fault set 4, clearly deform extensional veins belonging to fault set 2 and are therefore, at least locally, younger than this set. Because fault set 3 is spatially separated from the other two fault sets, cross-cutting relationships have not been described and the age of this fault set relative to the other two is not known.

All three post-folding fault sets (i.e. 2, 3, and 4) play an important role in the formation and geometry of the Rawil depression. As noted in "Geological setting: the Rawil depression", this depression was regarded as either being symmetric (e.g. Burkhard 1988a) or asymmetric (e.g. Dietrich 1989a), depending on which features were used to describe the depression. Schaub (1936) already realized that fault sets 2 and 4 could be responsible for this discrepancy. These fault sets have a predominantly NE-side up sense of movement. The accumulated displacement

along these faults produces an overall uplift of all units north-east of the Rawil pass and therefore shifts the centre of the depression, as defined by the tectonic units, south-westward from the Wildstrubel-Gemmi area toward the Rawil pass area. Schaub (1936) assigned these faults to a late brittle increment of uplift of the Aar massif that followed an earlier and more "ductile" uplift of the Aiguilles Rouge and Aar massifs.

Burkhard (1988a) not only considered the vertical displacement along fault set 4 but also the dextral strike-slip component. He interpreted the faults of set 4 as the surface expression of a dextral wrench-zone in the underlying basement. In an alternative model, Dietrich (1989a, b) and Ramsay (1989) interpreted fault sets 2 and 4 to be the expression of a pronounced fold-axis-parallel stretching phase, which occurred due to a change in the direction of overthrust shear late in the deformation history. The direction of shear was interpreted to rotate anti-clockwise from N-S to NW-SE (Dietrich and Durney 1986) to SW-NE (Dietrich 1989a, b). According to them, this rotation led to the formation of the arc of the western Alps, and was responsible for the late regional orogen-parallel extension, and in turn for the development of the Aiguilles Rouges and Aar culminations and the intervening Rawil depression. In contrast, Steck (1984), Burkhard (1986, 1988a, b), Mancktelow (1990, 1992), Hubbard and Mancktelow (1992) and Steck and Hunziker (1994) all considered the late NE-SW stretching to represent a true orogen-parallel extensional event, with the Neogene Rhone-Simplon fault zone as its main expression.

Today, the Rhone Valley and the southern Rawil depression belong to one of the seismically most active regions in Switzerland (Maurer et al. 1997; Delacou et al. 2004; Ustaszewski and Pfiffner 2008). Seismogenic faults interpreted from earthquake focal mechanisms strike ENE-WSW to WNW-ESE, with dominant dextral strike-slip and minor normal components and with epicentres at depths of <15 km. The inferred σ_1 plunges $\sim 30°$ towards NW, with σ_3 sub-horizontal and striking NE-SW (Maurer et al. 1997; Delacou et al. 2004; Ustaszewski and Pfiffner 2008). All three Neogene fault sets could have been active under this current stress field, which implies that the same mechanisms that formed these fault zones in the past may still persist at depth.

Conclusions

Our study shows that brittle faults in the Rawil depression can be assigned to four different fault sets, with one set formed before and during emplacement of the Helvetic nappes and three fault sets formed after emplacement of the Helvetic nappes. The three younger fault sets may all be involved in the formation of the Rawil depression and could be still active under the current stress field.

The Rezli fault zones are very well exposed examples of the prominent WNW-ESE striking set of faults in the centre of the Rawil depression. These faults dip moderately to the south-southwest and have an oblique slip vector with S-side-down and dextral sense of movement. The Rezli fault zones cut through different sedimentary protoliths such as limestones, bedded marls and limestones, marls and sandstones. They have a complex internal architecture that strongly depends on the lithology in which they developed. Whereas limestones and sandstones deform in a brittle manner, typically with the development of cataclasites and breccias (in the sandstones), marls and interbedded marls and limestones deform more ductilely along anastomosing shear zones, accompanied by pressure solution seams and veins. Common veins and calcite-cemented fault rocks indicate the strong involvement of fluids during faulting. Our detailed field study describes the internal geometry of fault zones which could act as models for similarly oriented seismogenic faults currently active at deeper levels in the same area.

Acknowledgments This paper is dedicated to the memory of Martin Burkhard, who initiated this project but tragically died before the field work could begin. Support from Swiss Nationalfonds Project no. 200021-109519 is gratefully acknowledged, as is material support from the University of Neuchâtel and the ETH Zurich. Bas den Brok is thanked for many discussions and a visit in the field. Geoffrey Milnes, Paul Bosshart and Jon Mosar are thanked for thorough and constructive reviews.

References

Anderson, E. M. (1951). *The dynamics of faulting*. London: Oliver and Boyd, Ltd.

Badoux, H. (1959). Atlasblatt St. Léonard. *Geologischer Atlas der Schweiz*, 1:25 000.

Badoux, H. (1962). Atlasblatt Lenk. *Geologischer Atlas der Schweiz*, 1:25 000.

Ballance, P. F. & Reading, H. G. (1980). Sedimentation in Oblique-Slip Mobile Zones. International Association of Sedimentologists, Special Publication 4, 265 pp.

Basile, C., & Brun, J. P. (1999). Transtensional faulting patterns ranging from pull-apart basins to transform continental margins: An experimental investigation. *Journal of Structural Geology, 21*, 23–37.

Bistacchi, A., Eva, E., Massironi, M., & Solarino, S. (2000). Miocene to Present kinematics of the NW-Alps: Evidences from remote sensing, structural analysis, seismotectonics and thermochronology. *Journal of Geodynamics, 30*, 205–228.

Bistacchi, A., & Massironi, M. (2000). Post-nappe brittle tectonics and kinematic evolution of the north-western Alps: An integrated approach. *Tectonophysics, 327*, 267–292.

Bonson, C. G., Childs, C., Walsh, J. J., Schöpfer, M. P. J., & Carboni, V. (2007). Geometric and kinematic controls on the internal structure of a large normal fault in massive limestones: The Maghlaq Fault, Malta. *Journal of Structural Geology, 29*, 336–354.

Bott, M. H. P. (1959). The mechanics of oblique slip faulting. *Geological Magazine, 96*, 109–117.

Braathen, A., Tveranger, J., Fossen, H., Skar, T., Cardoso, N., Semshaug, S. E., et al. (2009). Fault facies and its application to sandstone reservoirs. *American Association of Petroleum Geologists Bulletin, 93*, 891–917.

Burkhard, M. (1986). L'Helvetique de la bordure occidentale du Massif de l'Aar. Unpublished PhD thesis, University of Neuchatel.

Burkhard, M. (1988a). L'Hélvetique de la bordure occidentale du massif de l'Aar (évolution tectonique et métamorphique). *Eclogae Geologicae Helvetiae, 81*, 63–114.

Burkhard, M. (1988b). Horizontalschnitt des Helvetikums der Westschweiz auf 2500 m zwischen Mt. Blanc- und Aarmassiv (Rawil-Depression). Geologische Berichte Nr. 4, Landeshydrologie und -geologie, Bern, 34 pp.

Burkhard, M., & Kerrich, R. (1988). Fluid regimes in the deformation of the Helvetic nappes, Switzerland, as inferred from stable isotope data. *Contributions to Mineralogy and Petrology, 99*, 416–429.

Caine, J. S., Evans, J. P., & Forster, C. B. (1996). Fault zone architecture and permeability structure. *Geology, 24*, 1025–1028.

Champagnac, J. D., Sue, C., Delacou, B., & Burkhard, M. (2004). Brittle deformation in the inner NW Alps: From early orogen-parallel extrusion to late orogen-perpendicular collapse. *Terra Nova, 16*, 232–242.

Childs, C., Watterson, J., & Walsh, J. J. (1996). A model for the structure and development of fault zones. *Journal of the Geological Society of London, 153*, 337–340.

Christie-Blick, N., & Biddle, K. (1985). Deformation and basin formation along strike-slip faults. In K. Biddle & N. Christie-Blick (Eds.), *Strike-slip deformation, basin formation and sedimentation*. Society of Economic Paleontologists and Mineralogists, Special Publication 37, pp. 1–34.

Cobbold, P. R. (1976). Mechanical effects of anisotropy during large finite deformations. *Bulletin de la Société Géologique de France, 18*, 1497–1510.

Cowan, D. S. (1999). Do faults preserve a record of seismic slip? A field geologist's opinion. *Journal of Structural Geology, 21*, 995–1001.

Crider, J. G., & Peacock, D. C. (2004). Initiation of brittle faults in the upper crust: A review of field observations. *Journal of Structural Geology, 26*, 691–707.

Delacou, B., Sue, Ch., Champagnac, J.-D., & Burkhard, M. (2004). Present-day geodynamics in the bend of the western and central Alps as constrained by earthquake analysis. *Geophysical Journal International, 158*, 753–774.

Dietrich, D. (1989a). Fold-axis parallel extension in an arcuate fold-and-thrust belt: The case of the Helvetic nappes. *Tectonophysics, 170*, 183–212.

Dietrich, D. (1989b). Axial depressions and culminations in the evolution of the Helvetic chain. *Schweizerische Mineralogische und Petrographische Mitteilungen, 69*, 183–189.

Dietrich, D., & Casey, M. (1989). A new tectonic model for the Helvetic nappes. In M. P. Coward, D. Dietrich & R. G. Par (Eds.), *Alpine tectonics*. Geological Society of London Special Publication 45, pp. 47–63.

Dietrich, D., & Durney, D. W. (1986). Change of direction of overthrust shear in the Helvetic nappes of western Switzerland. *Journal of Structural Geology, 8*, 389–398.

Dietrich, D., McKenzie, J. A., & Song, H. (1983). Origin of calcite in syntectonic veins as determined from carbon-isotope ratios. *Geology, 11*, 547–551.

Faulkner, D. R., Lewis, A. C., & Rutter, E. H. (2003). On the internal structure and mechanics of large strike-slip fault zones: Field observations of the Carboneras fault in southeastern Spain. *Tectonophysics, 367*, 235–251.

Ferraccioli, F., & Bozzo, E. (2003). Cenozoic strike-slip faulting from the eastern margin of the Wilkes Subglacial Basin to the western margin of the Ross Sea Rift: An aeromagnetic connection. In F. Storti, R. E. Holdsworth & F. Salvini (Eds.), *Intraplate strike-slip deformation belts*. Geological Society of London Special Publication 210, pp. 109–133.

Föllmi, K. B., & Gainon, F. (2008). Demise of the northern Tethyan Urgonian carbonate platform and subsequent transition towards pelagic conditions: The sedimentary record of the Col de la Plaine Morte area, central Switzerland. *Sedimentary Geology, 205*, 142–159.

Franck, P., Wagner, J. J., Escher, A., & Pavoni, N. (1984). Evolution des contraintes tectoniques et sismicité dans la région du col du Sanetsch, Alpes valaisannes hélvetiques. *Eclogae Geologicae Helvetiae, 77*, 383–393.

Frey, M., & Mählmann, R. F. (1999). Alpine metamorphism of the Central Alps. *Schweizerische Mineralogische und Petrographische Mitteilungen, 79*, 135–154.

Furrer, H. (1938). Geologische Untersuchungen in der Wildstrubelgruppe, Berner Oberland. Mitteilungen der Naturforschenden Gesellschaft Bern, pp. 35–177.

Furrer, H. (1956). Atlasblatt Gemmi. *Geologischer Atlas der Schweiz*, 1:25 000.

Furrer, H., & Hügi, T. (1952). Telemagmatischer Gang im Nummulitenkalk bei Trubeln westlich Leukerbad (Kanton Wallis). *Eclogae Geologicae Helvetiae, 45*, 41–51.

Grosjean, G., Sue, Ch., & Burkhard, M. (2004). Late Neogene extension in the vicinity of the Simplon fault zone (central Alps, Switzerland). *Eclogae Geologicae Helvetiae, 97*, 33–46.

Günzler-Seiffert, H. (1952). Alte Brüche im Kreide/Tertiär-Anteil der Wildhorndecke zwischen Rhone und Rhein. *Geologische Rundschau, 40*, 211–239.

Hausegger, S., Kurz, W., Rabitsch, R., Kiechl, E., & Brosch, F. J. (2009). Analysis of the internal structure of a carbonate damage zone: Implications for the mechanisms of fault breccia formation and fluid flow. *Journal of Structural Geology*. doi: 10.1016/j.jsg.2009.04.014.

Heim, A. (1921). Geologie der Schweiz, Band II, Tauchnitz, Leipzig.

Henry, C. D., Faulds, J. E., & dePolo, C. M. (2007). Geometry and timing of strike-slip and normal faults in the northern Walker Lane, northwestern Nevada and northeastern California: Strain partitioning or sequential extension and strike-slip deformation? In A. B. Till, S. M. Roeske, J. C. Sample & D. A. Foster (Eds.), *Exhumation associated with continental strike-slip fault systems*, Geological Society of America Special Paper 434, pp. 59–79.

Hubbard, M., & Mancktelow, N. (1992). Lateral displacement during Neogene convergence in the western and central Alps. *Geology, 20*, 943–946.

Huerta, A. D., & Rodgers, D. W. (1996). Kinematic and dynamic analysis of a low-angle strike-slip fault: The Lake Creek fault of south-central Idaho. *Journal of Structural Geology, 18*, 585–593.

Huggenberger, P., & Aebli, H. (1989). Bruchtektonik und Blattverschiebungen im Gebiet des Rawil-Passes; Resultat einer E-W gerichteten dextralen Schwerbewegung im kristallinen Untergrund? *Schweizerische Mineralogische und Petrographische Mitteilungen, 69*, 173–180.

Jebrak, M. (1997). Hydrothermal breccias in vein-type ore deposits: A review of mechanisms, morphology and size distribution. *Ore Geology Reviews, 12*, 111–134.

Kelly, P. G., Sanderson, D. J., & Peacock, D. C. P. (1998). Linkage and evolution of conjugate strike-slip fault zones in limestones of Somerset and Northumbria. *Journal of Structural Geology, 20*, 1477–1493.

Kocher, T., & Mancktelow, N. S. (2006). Flanking structure development in anisotropic viscous rock. *Journal of Structural Geology, 28*, 1139–1145.

Kurz, W., Imber, J., Wibberley C. A. J., Holdsworth, R. E., & Collettini, C. (2008). The internal structure of fault zones: Fluid flow and mechanical properties. In C. A. J. Wibberley et al. (Eds.), *The internal structure of fault zones: Implications for mechanical and fluid flow properties*. Geological Society of London Special Publication 299, pp. 1–3.

Lee, H. K., & Kim, H. S. (2005). Comparison of structural features of the fault zone developed at different protoliths: Crystalline rocks and mudrocks. *Journal of Structural Geology, 27*, 2099–2112.

Levato, L., Sellami, S., Epard, J.-L., Pruniaux, B., Olivier, R., Wagner, J.-J., et al. (1994). The cover-basement contact beneath the Rawil axial depression (western Alps): True amplitude seismic processing, petrophysical properties, and modelling. *Tectonophysics, 232*, 391–409.

Mancktelow, N. S. (1985). The Simplon Line: A major displacement zone in the western Lepontine Alps. *Eclogae Geologicae Helvetiae, 78*, 73–96.

Mancktelow, N. S. (1990). The Simplon Fault Zone. Beiträge zur geologischen Karte der Schweiz [Neue Folge] 163, 74 pp.

Mancktelow, N. S. (1992). Neogene lateral extension during convergence in the Central Alps: Evidence from interrelated faulting and backfolding around the Simplonpass (Switzerland). *Tectonophysics, 215*, 295–317.

Masson, H. (1988). Les decrochements de la vallee du Rhone. In Heitzmann, P. (Ed.), NFP 20 Bulletin 6, Allgemeine Mitteilungen, pp. 40–41.

Maurer, H. R., Burkhard, M., Deichmann, N., & Green, A. G. (1997). Active tectonism in the central Alps: Contrasting stress regimes north and south of the Rhone Valley. *Terra Nova, 9*, 91–94.

Pavoni, N. (1980). Comparison of focal mechanisms of earthquakes and faulting in the Helvetic zone of the Central Valais, Swiss Alps. *Eclogae Geologicae Helvetiae, 73*, 551–558.

Peacock, D. C. P. (2008). Architecture, gods and gobbledygook. *Journal of Structural Geology, 30*, 687–688.

Price, N. J. (1966). *Fault and joint development in brittle and semi-brittle rock* (p. 176). Oxford: Pergamon Press.

Ramsay, J. G. (1981). Tectonics of the Helvetic nappes. In K. McClay & N. J. Price (Eds.), *Thrust and nappe tectonics*. Geological Society of London Special Publication 9, pp. 293–309.

Ramsay, J. G. (1989). Fold and fault geometry in the western Helvetic nappes of Switzerland and France and its implication for the evolution of the arc of the western Alps. In M. P. Coward et al. (Eds.), *Alpine tectonics*. Geological Society of London Special Publication 45, pp. 33–45.

Schaub, H. P. (1936). Geologie des Rawilgebietes (Berner Alpen). *Eclogae Geologicae Helvetiae, 29*, 337–407.

Scholz, C. H. (1988). The brittle-plastic transition and the depth of seismic faulting. *Geologische Rundschau, 77*, 319–328.

Schöpfer, M. P. J., Childs, C., Walsh, J. J., Manzocchi, T., & Koyi, H. A. (2007). Geometrical analysis of the refraction and segmentation of normal faults in periodically layered sequences. *Journal of Structural Geology, 29*, 318–335.

Sibson, R. H. (1977). Fault rocks and fault mechanisms. *Journal of the Geological Society of London, 133*, 191–213.

Sibson, R. H. (1986a). Earthquakes and rock deformation in crustal fault zones. *Annual Reviews in Earth Planetary Science, 14*, 149–175.

Sibson, R. H. (1986b). Brecciation processes in fault zones: Inferences from earthquake rupturing. *PAGEOPH, 124*, 159–175.

Sibson, R. H. (1990). Conditions for fault-valve behaviour. In R. J. Knipe & E. H. Rutter (Eds.), *Deformation mechanisms, rheology and tectonics*. Geological Society of London Special Publication 54, pp. 15–28.

Sibson, R. H. (1994). Crustal stress, faulting and fluid flow. In Parnell, J. (Ed.), *Geofluids: Origin, migration and evolution of fluids in sedimentary basins*. Geological Society of London Special Publication 78, pp. 69–84.

Snoke, A. W., Tullis, J., & Todd, V. R. (1998). *Fault-related rocks. A photographic atlas*. Princeton University Press, 629 pp.

Steck, A. (1984). Structures de déformation tertiaires dans les Alpes centrales (transversale Aar-Simplon-Ossola). *Eclogae Geologicae Helvetiae, 77*, 55–100.

Steck, A. (1999). Feuille Col du Pillon, Carte tectonique des Alpes de Suisse occidentale, *1*, 100'000.

Steck, A., & Hunziker, J. (1994). The tertiary structural and thermal evolution of the Central Alps—compressional and extensional structures in an orogenic belt. *Tectonophysics, 238*, 229–254.

Tarasewicz, J. P. T., Woodcock, N. H., & Dickson, J. A. D. (2005). Carbonate dilation breccias: Examples from the damage zone to the Dent fault, northwest England. *Geological Society of America Bulletin, 117*, 736–745.

Ustaszewski, M., Herwegh, M., McClymont, A., Pfiffner, A. O., Pickering, R., & Preusser, F. (2007). Unravelling the evolution of an Alpine to post-glacially active fault in the Swiss Alps. *Journal of Structural Geology, 29*, 1943–1959.

Ustaszewski, M., & Pfiffner, O. A. (2008). Neotectonic faulting, uplift and seismicity in the Central and Western Swiss Alps. In S. Sigmund et al. (Eds.), *Tectonic aspects of the Alpine-Carpathian-Dinaride System*. Geological Society of London Special Publication 298, pp. 231–249.

Wibberley, C. A. J., Yielding, G., & di Toro, G. (2008). Recent advances in the understanding of fault zone internal structure: A review. In C. A. J. Wibberley et al. (Eds.), *The internal structure of fault zones: Implications for mechanical and fluid flow properties*. Geological Society of London Special Publication 299, pp. 5–33.

Willemse, E. J. M., Peacock, D., & Aydin, A. (1997). Nucleation and growth of strike-slip faults in limestones from Somerset, UK. *Journal of Structural Geology, 19*, 1461–1477.

Williams, A. (1958). Oblique-slip faults and rotated stress systems. *Geological Magazine, 95*, 207–218.

Wilson, P. (2008). Comment on 'Architecture, gods and gobbledygook'. *Journal of Structural Geology, 30*, 1614.

Woodcock, N. H., & Fischer, M. (1986). Strike-slip duplexes. *Journal of Structural Geology, 8*, 725–735.

Woodcock, N. H., Omma, J. E., & Dickson, J. A. D. (2006). Chaotic breccia along the Dent Fault, NW England: Implosion or collapse of a fault void? *Journal of the Geological Society of London, 163*, 431–446.

Woodcock, N. H., Sayers, N. J., & Dickson, J. A. D. (2008). Fluid flow history from damage zone cements near the Dent and Rawthey faults, NW England. *Journal of the Geological Society of London, 165*, 829–837.

Wu, J. E., McClay, K., Whitehouse, P., & Dooley, T. (2009). 4D analogue modelling of transtensional pull-apart basins. *Marine and Petroeum Geology, 26*, 1608–1623.